

APPENDIX II. IN-SITU CHARACTERIZATION OF THE THERMAL DISTRIBUTION SYSTEM
IN A LARGE COMMERCIAL BUILDING

Craig Wray, Darryl Dickerhoff, Nance Matson, Duo Wang, and Rick Diamond
Lawrence Berkeley National Laboratory
Berkeley, California

Martha Brook, Project Manager
PIER Buildings End-Use Energy Efficiency Program, Nancy Jenkins, Lead

PIER Contract Number: 500-98-026

December 6, 2002

In-Situ Characterization of the Thermal Distribution System in a Large Commercial Building

Summary

This appendix describes our recent in-situ characterization activities in a 25 story office building in Sacramento, California; we carried out this work as part of the PIER “Thermal Distribution Systems in Commercial Buildings” project. Our review of the literature and our previous research has found very little characterization of the actual performance of thermal distribution systems in large commercial buildings. Our initial duct leakage assessment using conventional industry methods indicated that the duct system was leaky, but this was only part of the story. By conducting more sophisticated duct leakage airflow diagnostics, we determined that the actual airflow through these leaks was small (about 5% at operating conditions), and consequently less significant. Our test building showed every indication of a “tight” thermal distribution system: good application of mastic, metal bands at joints, and overall high quality installation. In order to demonstrate the impact of duct leakage, we introduced measured leaks and monitored the impact of these controlled leaks to determine their impact on the HVAC system energy consumption.

The principal outcome from this project is that the energy impact of duct leakage in large commercial buildings can be substantial. By adding 15% duct leakage to make a total of 20% at operating conditions, we found that the added leakage leads to an increase in air-handler supply fan power of up to 37%, and an overall increase in total fan power (air-handler supply fans plus induction fans) of up to 26%. The total fan power increase is lower because the added duct leakage causes induction fans to operate less often.

Previous simulations (Franconi et al. 1998) have suggested that the energy impacts of 20% duct leakage are larger: on the order of 60% to 70% of the total fan energy consumption. However, the duct leakage fraction in the simulations is normalized by nominal design supply airflow rather than by operating supply airflow. Redefining our duct leakage fraction to match the definition used in the simulations means that the duct leakage that we added was about 10% of the nominal design supply airflow. Given that our leakage fractions were about 50% of those used in the simulations, and assuming that fan power is somewhere between a quadratic and cubic function of airflow, our measurements are consistent with the simulation results.

The remainder of this appendix provides a general description of the test building and its thermal distribution system; a description of our monitoring and diagnostic activities; a summary of our preliminary duct leakage findings; a description of the HVAC system airflow diagnostics that we carried out prior to and during our duct leakage intervention tests; and a summary of our HVAC fan power measurements, and other findings.

Building and Thermal Distribution System – General Description

For our large commercial building characterization and duct leakage intervention study, we selected an office building in Sacramento, California. Eley Associates is also studying this building for a different PIER project (New Buildings Institute, Element 3: Integrated Design of Large Commercial HVAC Systems), so it offers the potential for collaboration between our efforts. The building, first occupied in April 2001, has 25 stories and a total floor area of 955,000 ft². Our study focused on two floors with similar occupancy and use (each

approximately 29,000 ft² in floor area). We extensively characterized the HVAC system operation on the intervention (17th) floor before installing duct leaks on this floor; we used the 16th floor as a control floor (i.e., with no changes to the HVAC system as a basis for comparison to the intervention floor).

Each floor has four separate air-handlers, with two nominal 15,000 cfm, 15 hp supply air-handlers per floor and two nominal 10,000 cfm, 5 hp relief air-handlers per floor. Each pair of supply and relief air-handlers is located in a separate mechanical room at the northeast and northwest corners of each floor, and each air-handler uses an EMCS-controlled variable-frequency-drive. Each supply air-handler is a draw-through packaged unit equipped with an air mixing chamber, a filter section, a hot-water air preheat coil, a chilled-water air cooling coil, and a backward-curved plug fan. Each relief air-handler uses a backward-curved tube-axial centrifugal fan. A central plant with boilers and three chillers (rated 1200, 800 and 300 tons) supplies the appropriate air-handler coils with cold and hot water.

Together, the two supply air-handlers on each floor serve a single-duct VAV system supply loop that in turn serves 34 VAV boxes on the intervention floor and 38 boxes on the control floor (see Figure II-1). The difference between the number of zones on the two floors is due to slight changes in room configuration, and does not affect our findings. A single duct-static-pressure-sensor in each loop is located at the farthest point from the air-handlers. The 13 perimeter VAV boxes on the intervention floor and the 14 perimeter boxes on the control floor have discharge electric reheat coils (750 to 2,500 W, staged) and are parallel-fan-powered (1/6 and 1/4 hp induction fans), with the fans drawing their induction air from the ceiling plenum return through a pleated filter and discharging into the primary air section of the box through an adjustable fixed-stop gravity backdraft damper. The core VAV boxes have no reheat and no induction fans. Each VAV box inlet has a flow grid located immediately upstream of its EMCS-controlled primary air damper.

In total, the VAV boxes on the intervention floor serve 103 supply grilles, each with a manual volume damper located near the branch takeoff. Most supply grilles use 2' x 2' perforated-face grilles and discharge in multiple directions; exceptions are the wall grilles in the two electrical rooms, a discharge with no grille in the communications equipment room, and the linear slot diffusers in the two main elevator lobbies. The 2' x 2' grilles sit in the ceiling between T-bar sections, with a small gap between the grille edges and the T-bar sections.

With the exception of the elevator lobbies (portions of the slot diffusers also serve as return grilles), ceiling returns are 2' x 2' perforated-face grilles. The mechanical rooms are each connected to the ceiling space through a short return transfer duct, and serve as a large plenum from which the supply air-handler draws its return air through EMCS-controlled return dampers.

Outdoor air is ducted to each supply air-handler mixing box from a wall louver and through two parallel EMCS-controlled dampers: a minimum outdoor air damper and a larger economizer damper. Return air is exhausted directly from each mechanical room to outdoors by the relief air-handler, as needed to control indoor-outdoor pressure difference for the floor. The indoor pressure appears to be referenced to the outdoor pressure at the building roof.

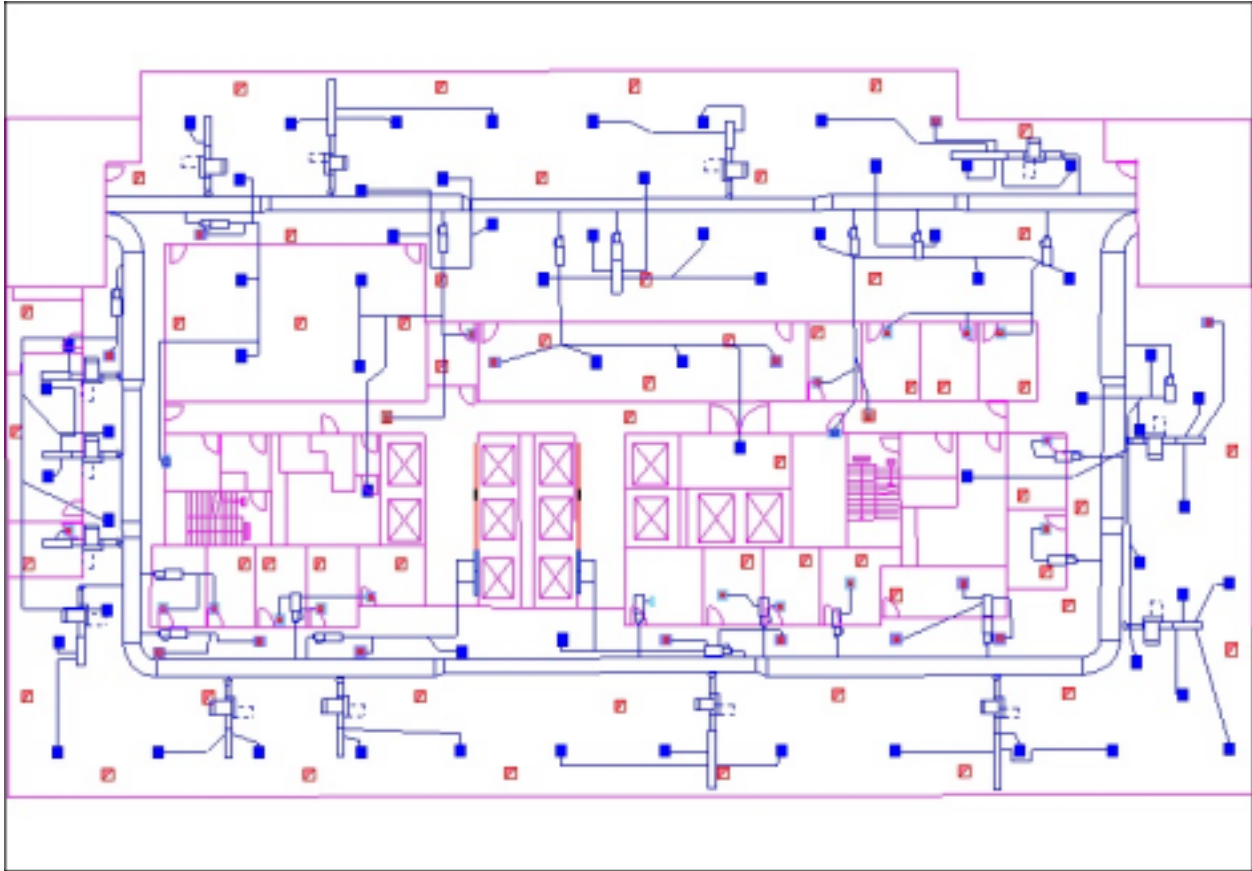


Figure II-1. Duct layout for intervention floor. The control floor's duct layout is similar.

All ducts are constructed from sheet metal, except for the flexible duct connections to the supply grilles. All joints are covered externally with mastic. We also found mastic covering the inside of branch duct connections to the VAV box plenums. Except in the mechanical rooms and in the ceiling space near those rooms where there is internal insulation, external insulation with a vapor barrier covers the ducts.

HVAC System Operation - Cooling Mode: The building operated in cooling mode during our duct leakage intervention study. In this mode, the EMCS puts each floor's air handling system through a short smoke control system check between about 2:00 a.m. and 2:30 a.m.

If pre-cooling is not needed, the HVAC systems are put into occupied mode around 4:00 a.m. and the systems run to maintain zone temperature conditions until 6:00 p.m. If pre-cooling is needed (dictated by building and outdoor temperatures measured at midnight), the corresponding HVAC system is put into economizer mode (outdoor air dampers fully open) and the air-handler supply fans are operated for pre-cooling. The relief fans run as needed to maintain building pressures.

During the occupied mode, the discharge duct temperature measured at the outlet of the air-handlers is used to control the heating and cooling valves serving the coils upstream of the air handler supply fan. The temperatures measured by the EMCS zone thermostats are used to determine the corresponding amount of primary air needed from the main loop through the VAV

box to each zone. The primary air damper is adjusted accordingly. For the powered boxes, the induction fans are energized if the primary airflow is less than 40% of the damper’s throttling range maximum set point.

Building Monitoring

We extensively monitored the intervention and control floors to characterize HVAC system operation and to determine the impact of duct leakage on fan energy consumption. The monitoring occurred over the period from November 2001 to early August 2002. Much of the monitoring in advance of our duct leakage intervention tests during the summer of 2002 was used to support our characterization diagnostic tests, but was also useful to troubleshoot the operation of our monitoring equipment and to validate the data being collected using the building’s Energy Management Control System (EMCS). Our monitoring using the EMCS involved recording data for 232 measurement points. In addition, we installed 96 temperature, relative humidity, pressure, and power monitoring points. Table II-1 summarizes these 328 points.

Table II-1. Monitoring point summary.

	<i>EMCS Monitoring</i>	<i>LBNL Installed Monitoring</i>
<i>Supply Fans</i>		Electricity consumption, pressure (airflow)
<i>Relief Fans</i>		Electricity consumption
<i>Outdoor Air Supply</i>	Minimum outdoor airflow; economizer damper position	Air temperature; relative humidity
<i>Return Air</i>	Damper position; air temperature; relative humidity	Pressure (airflow); air temperature; relative humidity
<i>Air Handler Cabinet</i>	Supply air temperature (after fan)	Supply air temperature and relative humidity (after supply fan and before heating coil); air temperature between cooling coil and supply fan
<i>Zones (All)</i>	Zone air temperature, primary airflow	
<i>Zones (All with Induction Fans and Heaters)</i>	Induction fan status (off / on); box reheat status (off / 1 st stage / 2 nd stage)	
<i>Zones (Detailed)</i>		Air temperature and static pressure before and after VAV box; total pressure after box; air temperature in VAV box before heater (where applicable); air temperature at inlet to induction fan (where applicable); supply air temperature at the farthest grille
<i>Zones (Partial Detail)</i>		Supply air temperature at the farthest grille
<i>Outdoor Conditions</i>	Air temperature; relative humidity	
<i>Miscellaneous Temperatures and Pressures</i>	Static pressure in supply loop (one location per floor); indoor-outdoor static pressure difference	Static pressure in far supply loop corners; ceiling plenum air temperature (two locations, intervention floor)

Zones: On the zone level, the building’s EMCS was set to record zone temperatures and all VAV box primary airflows on the control and intervention floors. For the VAV boxes with induction fans, the EMCS also recorded induction fan status (on / off) and box heater status (off / stage 1 /

stage 2). We measured the induction fan power as a function of VAV box primary airflow reported by the EMCS. The EMCS primary airflow and fan status data were then used to calculate induction fan energy over the test period. We also measured the heater power for each powered VAV box.

We monitored four VAV boxes on the intervention floor (North and South locations, two with induction fans and two without) in detail using Onset Hobo Pro temperature sensors and two Energy Conservatory 8-channel Automatic Performance Testing (APT) systems. Temperatures were measured before the VAV box, inside the box before the heater (where applicable), after the VAV box, and at the farthest supply grille. The APTs were used to measure and record duct static pressures before and after the VAV boxes, as well as downstream duct total pressure.

We also installed Onset Hobo Pro temperature sensors at the farthest supply grille for ten other VAV boxes: four on the intervention floor, representing East and West orientations, with and without induction fans and heaters; and eight on the control floor, two on each of the four orientations, with and without induction fans and heaters.

Mechanical Rooms: Onset Hobo Pro temperature/relative humidity (RH) sensors were installed to monitor thermal conditions in the outdoor air intakes, at the return dampers (for calibrating EMCS data), before the heating coils, immediately after the cooling coils (before the system fans), and after the system fans. These thermal data were primarily collected to support our airflow diagnostics and monitoring, but are also useful for future evaluations of floor-by-floor heating and cooling coil demand imposed on the central plant. Pressure transducers (Setra 264, Modus T10, and Validyne DP103) were used to translate the supply grid and return grid pressures and the supply and relief fan static pressures to millivolt signals for the Datataker 50 data logger. Ohio Semitronics WL45R electric power transducers were installed and connected to the Datataker 50 to monitor supply and relief fan electricity usage. Each electric power transducer produces a pulse output that the data logger records on a minute by minute basis.

Outdoor Conditions: The EMCS recorded outdoor temperature and relative humidity, as well as calculated enthalpy, during the test period. We also installed two Onset Hobo Pro temperature/RH sensors in the outdoor air plenums on the intervention floors so that we could later compare the EMCS data to our measurements.

Additional Data Collection for Others: Following our monitoring period, Eley Associates and Taylor Engineering plan to conduct part of their PIER research project in the same building. To better facilitate their data needs, we installed additional measuring equipment in the intervention and control floor mechanical rooms: pressure (static across the supply and relief fans) and relief fan airflow. We also added zone damper positions to the points being monitored by the EMCS.

Data Synchronization: We used the duct static pressure signal at the system test time (~2:30 am) to synchronize the EMCS data to the data logger supply fan power and airflow data. The EMCS data were recorded at one, two, or five minute intervals, depending on the point being monitored. We interpolated to estimate missing values. For longer time periods (up to 60 observations once or twice a week during EMCS data download by building staff), we interpolated based on two values: the average of the observations in the hour before the missing data and the average of the observations in the hour after the missing data. This approach did not change the results significantly. We used the factory calibration for the power transducers and calibrated the airflow measuring equipment as discussed in the “Characterization of HVAC

System Airflows” section, which follows. The outdoor air temperatures and zone temperatures discussed in this report are as reported by the EMCS system.

Diagnostic Tests: Besides downloading and retrieving monitoring data, our main efforts during our approximately 30 field visits to the building included a number of diagnostic tests to characterize the system and study operational modes. These tests included:

Tracer gas measurements:

- Air-handler supply fans
- VAV box primary airflow grids

Pressure Diagnostics:

- Carried out static pressure traverses of air-handler supply fan plenum to determine the optimal location for static pressure taps used to measure static pressure rises across the supply fan (for Eley/Taylor project).
- Determined main loop static pressure profiles at different operating conditions to assess uniformity of pressure and to identify limits for VAV box opening that allow HVAC system to maintain loop set point static pressure.
- Measured pressure differences across doors to corridors, bathrooms, electrical rooms to validate airflow diagnostic anomalies.
- Measured static pressures in VAV boxes and at installed downstream leakage sites as a function of the EMCS-reported VAV box primary airflow.
- Measured operating pressures at installed downstream and upstream leakage sites to support leakage airflow calculations.

Flow Hood Measurements:

- Used powered flow hoods to determine the total airflow exiting the supply grilles (sum of supply grille airflows).
- Used powered and commercially available flow hoods on a sample of grilles to test flow hood repeatability and to assess hood usability and accuracy for a rapid duct leakage screening method.

Leakage Diagnostics:

- Carried out component and total duct leakage tests at all detail and partial detail VAV boxes on the intervention floor. This included determining component leakage areas of the VAV box, induction fan damper, ducts, and grilles.
- Measured duct leakage upstream of the VAV boxes by fully closing all VAV primary air dampers and using a calibrated fan and flowmeter at the air-handler supply fan plenum.
- Conducted HVAC system and VAV box inspections and measurements to develop plans to add calibrated leakage and to demonstrate leakage sealing using the multiple compact aerosol injector.
- Tested effectiveness of backer rod insulation to seal leaks at supply grille edges.

Diagnostics Using the EMCS:

- Set the individual VAV box primary airflow set point to zero: record the primary airflow that the EMCS reports and visually determine the actual position of all primary air dampers.
- Measured induction fan and heater power as a function of VAV box primary airflows (Base leakage case and downstream leakage case) (using Elite Pro power monitor).
- Carried out VAV box airflow capacity tests to determine the range of primary airflow set points (% of cooling maximum set points) that correspond to maintaining 1" w.c. in the main loop.

Diagnostics for Others:

- Modulated outdoor air / return air dampers for airflow tests. (Federspiel Controls)
- Maintained constant duct pressure for duct traverses. (Eley Associates / Taylor Engineering)
- Taught Taylor Engineering how to download monitoring data for their PIER project.

System Layout & Equipment Inspections:

- Verified and noted changes to duct layout as shown in plans.
- Developed detailed duct maps of four VAV boxes that we studied in detail and four partial zones on the intervention floor (lengths, sizes, location).
- Inspected equipment to verify measurement results.

Miscellaneous Calibrations:

- Calibrated pressure transducers.
- Installed physical filters on relief fan static pressure taps.
- Calibrated EMCS thermostat data with Onset Temperature Hobos (data collected to be analyzed as part of a future thermal analysis project).
- Calibrated analog airflow gauges on air-handler supply fans in support of a rapid duct leakage diagnostic.
- Used an aspirated temperature sensor to estimate the radiant component of temperature sensors downstream of powered VAV boxes, based on primary airflow, induction fan, and heater status.

Preliminary Assessment of Duct Leakage

To determine whether there was adequate leak-sealing potential for our retrofit study, we used duct pressurization techniques similar to those described by SMACNA (1985) to measure the leakage of six sample duct branches on the intervention floor, as well as the leakage of the main loop duct system on that floor. Table II-2 summarizes the results from those tests, using several different metrics to express the leakage. Duct surface areas in Table II-2 are based on field measurements of the ducts as they are actually installed.

Table II-2. “As Found” duct leakage based on duct pressurization tests.

VAV Box*	Number of Supply Grilles	ELA ₂₅ (cm ²)	Duct Surface Area (ft ²)	ELA ₂₅ / Surface Area (cm ² /m ²)	Leakage Class, C _L (cfm/100 ft ²)	Leakage Flow @ 1" w.c. (cfm)
1702	3	53	198	2.9	128	252
1704	2	53	152	3.7	183	278
1708	2	54	139	4.1	200	278
1712	3	51	243	2.3	120	292
1720	5	67	321	2.2	114	367
1729	5	163	291	6.0	282	821
Average**		56	210	3.1	149	294
Loop		52	5,076	0.1	6	309

* VAV boxes 1702 through 1712 are parallel fan-powered and have backdraft dampers at the fan discharge into the VAV box; the other two boxes (1720 and 1729) are unpowered and have no backdraft dampers.

** The averages in Table II-2 exclude Box 1729. That VAV box has two different, much leakier supply grilles (4 ft. long linear slot diffusers instead of 2 ft. square perforated-face multiple-throw diffusers).

Table II-2 indicates that the leakage class (C_L) for the tested branches (downstream of the primary air dampers, and including VAV box leakage at the induction fan air intake dampers) was approximately 114 to 282 cfm at 1 in. w.c. pressure per 100 ft² of duct surface area. This leakage is about mid-range compared to the leakage (C_L = 58 to 606 cfm per 100 ft²) of branch ducts that we have tested in other large commercial building systems (Xu et al. 2002).

The supply loop is very tight (C_L = 6 cfm / 100 ft²) in comparison to the branch ducts. This finding was not surprising given that the building is new and the main supply loop was well sealed with mastic. The supply loop includes all ducts between the supply fans and primary air dampers. Other systems that we have tested (Xu et al. 2002) have been leakier (C_L = 34 to 121 cfm/100 ft²).

Component Leakage Tests: Component leakage tests that we conducted on the six branches indicate that induction fan backdraft damper leakage, grille edge leakage, and slot diffuser boot leakage are the most significant components of the branch leakage area. Excluding Box 1729, which has the slot diffusers with higher leakage areas, the backdraft dampers are about 7 to 13% of the leakage area (ELA₂₅ of 4 to 7 cm²), while the grille edges are about 54 to 75% of the leakage area (ELA₂₅ of 29 to 51 cm²). The larger fractions for the dampers correspond to boxes supplying fewer grilles; the larger fractions for the grille edges correspond to branches with more grilles. Accounting for the number of grilles in each branch, the average backdraft damper and grille edge leakage area (ELA₂₅) is about 5 cm² and 12 cm² respectively. Due to the long perimeter of each grille (8 feet), the grille edge leakage is very sensitive to grille seating on the T-bar supports: this leakage can easily vary by a factor of two due to poor seating.

The two slot diffuser boots attached to one takeoff from Box 1729 are very leaky. With the edges of the other three grilles sealed, 78% of the leakage remained (ELA₂₅ of 128 cm²). Even after considerable sealing of the supply boots to the slot diffuser with tape, 44% of the leakage still remained. Almost half of the slot diffuser boots are difficult or impossible to seal, because of poor access to parts of the assemblies that are located adjacent to elevator shaft walls. Fortunately, there are only four slot diffusers on the entire floor.

The component leakage tests that we have carried out do not address duct leakage airflows. Those airflows depend on leakage area and pressure across the leak. Leaks at the induction fan backdraft dampers are at much lower pressure differences than in the main loop, and leaks at the grille edges are likely at even lower pressure differences. Based on our monitoring, the loop operates at a pressure of about 250 Pa; the branch pressures in the plenums downstream of the VAV boxes vary widely from about 0.2 Pa to 84 Pa, more so for some boxes than others, and depend on the positions of the primary air dampers and whether the induction fans are operating. Such a wide range of pressures is not helpful in determining duct leakage airflows. For example, using the pressure difference range of 0.2 to 84 Pa with the component leakage areas that we have measured and extrapolating to the entire system indicates that the total system leakage could be anywhere from 500 to 7,000 cfm (about 60% in the loop in the lower case, and about 60% at the 99 grille edges in the higher case, with only about 10 to 15% from the backdraft dampers and slot diffusers in either case).

If the grille edges have significant leakage airflows, then it makes sense to try to seal them. Unfortunately, the pressure differences across the grille edge leaks are practically impossible to directly measure in the field, so one cannot determine the grille leakage airflows based on leakage area. To circumvent this problem, we conducted diagnostic tests to assess the impact of sealing the grille edges on the airflow leaving the grilles. Using a powered flow hood, we measured grille airflows before and after sealing the grille edges for all five grilles of one unpowered VAV box (using closed-cell-foam round backer rod as a seal; taping the joints produces the same effects, but the rod is faster to install). The airflows from the grilles increased 23 cfm from an initial total of 1,507 cfm (1.5% increase); each grille airflow increased 2 to 8 cfm. The total increase of 1.5% is not significant, as it is within the measurement precision of our flow hood. In contrast, the leakage area of the VAV box downstream section (including the grille edges) decreased from 69 cfm₂₅ to 23 cfm₂₅ when the grille edges were sealed (67% reduction). Based on these results, it appears that even though the grille edges have significant leakage area, the effective pressures at the grille edges are very low, and there is no significant leakage airflow across these edges. Therefore, it does not seem worthwhile to further pursue sealing techniques for grille edges.

To further understand opportunities for duct leakage reduction, we carried out laboratory diagnostics on one fan-powered VAV box to evaluate VAV box component leakage areas. It appears that about 30% (5 cfm₂₅) of the box leakage is across the partition separating the primary air path from the induction fan inlet, with about 70% (3 cfm₂₅) of that at the fan backdraft damper. Our component leakage field tests indicated damper leakage could be 2 to 3 times greater than this value in other boxes, but it seems that damper leakage may not be a significant issue, particularly when there are only a few VAV boxes with such dampers. In any event, field retrofits to reduce backdraft damper leakage would be difficult because of limited access and aerosol sealing cannot be used to seal the damper edges (the damper needs to open when the induction fan is on). Providing a better sealing for the backdraft damper and partition appears to be a design and manufacturing issue more so than an installation or field retrofit issue.

Characterization of HVAC System Airflows

Although air leaks from supply ducts, is captured in the return air, and may be regained from a thermal viewpoint, the leakage airflow does not reach the conditioned spaces directly. To

maintain the main duct static air pressure at its set point, all leakage upstream of the VAV boxes must be made up by an increase in the supply fan airflow. Leakage downstream of the VAV boxes must be made up by supplying more air to the VAV boxes. To deliver more supply air, VAV box primary air dampers need to open further. Consequently, to maintain the main duct static pressure at its set point, an increase in the supply fan airflow is also needed to compensate for the downstream leakage airflows. The increase in the supply fan airflow in turn requires the supply fan speed to increase. Because the relationship between fan power and airflow is approximately a cubic function, the increase in supply airflow means that a large fraction of the supply fan power is used just to move the leaking air. Note that some of the thermal losses associated with duct leakage are not entirely recaptured during periods of economizer use, because relief fans discharge some of the return air directly to outdoors to maintain building envelope pressure differentials that would otherwise increase due to the increased outdoor airflows entering the building through the economizer.

Duct leakage airflows depends not only on leak size, but also on leak location, because the pressure difference at the leaks varies throughout a VAV system, particularly downstream of the VAV boxes. The pressure difference at each leak is determined by the airflows through the ducts and the airflow resistance of the duct system. Consequently, to understand duct leakage, one also needs to understand how airflows vary throughout the duct system. There are many HVAC system airflows of interest in this study: supply airflows, return airflows, outdoor airflows, VAV box primary airflows, VAV box induction airflows, supply grille airflows, and duct leakage airflows. The following sections describe in more detail how we determined each type of airflow.

HVAC System Airflow Calibrations and Diagnostics

Few HVAC system airflows on the intervention and control floors could be monitored using the Energy Management Control System (EMCS). The only airflows that could be monitored this way were the minimum outdoor airflows and the primary airflows entering each VAV box. We installed equipment to monitor supply fan and return airflows (the difference being total outdoor airflow, which includes economizer airflow). In particular, we installed equipment to measure the pressure difference across existing airflow grids (air-handler supply airflow) and across flow grids that we installed (return airflow). These pressure differences were then correlated to airflows by applying calibration equations that we developed.

We also made detailed airflow measurements for four VAV boxes: two have induction fans operating in parallel with the primary air; the other two are non-powered and have no induced airflow. We calibrated the primary inlet flow grid for each box and, for the boxes with fans, also measured the actual amount of induction airflow while varying the primary airflows. Obtaining these airflows with and without added downstream duct leakage was advantageous because the resulting data will support future analyses of the efficiency of the VAV units and their downstream duct sections under varying operating conditions and leakage configurations. The flow grid data have already been useful in assessing and rejecting various duct leakage sampling techniques that might use the EMCS airflow data to determine duct leakage airflows.

Calibration of the Supply Fan Flow Grids via Tracer Gas: Each supply fan (two on the control floor and two on the intervention floor) has an inlet airflow grid to measure the supply airflow, but none were connected to the EMCS system; each grid was instead connected only to an analog gauge that allows building engineering staff to determine airflow on a “snapshot”

basis. To monitor the supply airflow continuously (minute by minute), we installed pressure sensors connected to our data loggers and recorded the pressures that the airflow grid sees. Figure II-2 is a picture of a supply fan inlet with its flow grid.



Figure II-2. Air-handler supply fan inlet. Note the two vertical copper tubes that comprise the airflow station. A tube for lubricating the shaft bearing can also be seen, as well as one of the temperature sensors that we installed.

For each fan, to determine the relationship between the pressure difference across the supply fan flow grid and the airflow through the supply fan, we first calibrated the flow grid using a tracer gas technique that determines the airflow. The approach was to set the system for 100% outdoor air (with closed and sealed return air dampers). Sulfur hexafluoride¹ tracer gas was then injected into the duct system at a constant and measured rate immediately upstream of the cooling coil (which is upstream of the supply fan and downstream of the return and outdoor air inlets). A diffuse injection was accomplished by using a “soaker hose” spread out across the coil. The tracer gas concentration was monitored downstream of the fan before any duct branching, using a tracer gas analyzer calibrated at the measurement site. The airflow through the fan is given by Equation 1:

$$Q_{fan} = I / C \quad (1)$$

where Q_{fan} is the fan airflow ($[m^3_{air}]/s$), I is the tracer gas injection rate ($[m^3_{gas}]/s$), and C is the concentration of the tracer gas ($[m^3_{gas}]/[m^3_{air}]$).

¹ This tracer gas has been used extensively in past studies of other buildings. The engineering staff in the test building approved the tracer gas use after reviewing its “Material Safety Data Sheet” and after smelling the gas (no smell).

The major obstacle to tracer gas measurements of fan airflow (apart from equipment costs) is potentially poor mixing of tracer gas in the air stream between the tracer injection point and the downstream location where the tracer gas concentration is measured. Good mixing in our tests was confirmed by collecting and analyzing samples from multiple downstream locations inside the duct.

Uncertainties in the supply airflow measurements are due to uncertainties in the tracer gas injection rate, uncertainties in the tracer gas concentration, and uncertainties caused by sampling imperfectly mixed tracer gas in the air. With proper calibration and operation of the instruments, both uncertainties in the tracer gas injection rate and concentration can be as low as approximately 1% individually. Uncertainties due to an imperfect characterization of the well-mixed tracer concentration downstream of the injection point were about 2.5%.

By repeating the tracer gas tests at several different fan airflows, a curve fit was developed to determine the correlation between measured airflow (from the tracer gas) and grid pressure difference. The uncertainty in the curve fit is 2 to 3% of estimated fan airflow at the 95% confidence level. Consequently, the uncertainty of an airflow predicted from a measured pressure difference varies from 3 to 4%. Figure II-3 shows a typical calibration for a supply flow grid.

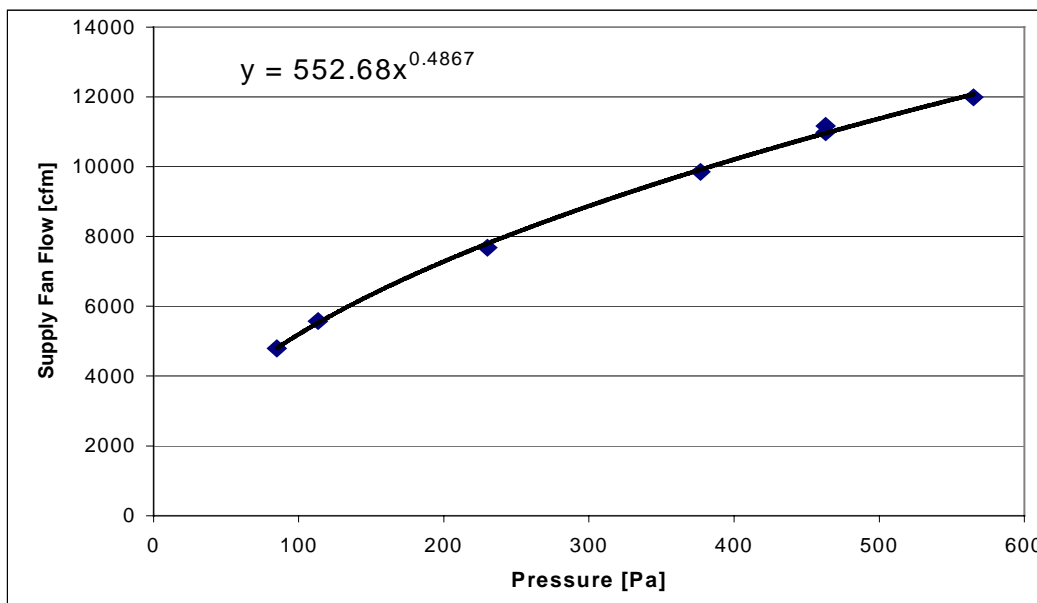


Figure II-3. Calibration for the intervention floor’s West supply flow grid.

Construction and Calibration of the Return Flow Grids: Although there was an airflow sensor connected to the EMCS to measure the minimum outdoor airflow for each supply fan, there was no existing measurement equipment in the building to measure return airflow or the total outdoor airflow entering the mixing box upstream of each supply fan (sum of the economizer airflow and the minimum outdoor airflow). Therefore, we monitored the return airflows by building, installing, and calibrating a new flow grid. We chose to measure the return airflow rather than the outdoor airflow because the return airflow was less likely to be affected by airflow non-uniformities: it did not have upstream duct work (the outdoor air ductwork had a 90

degree turn just upstream of the measurement section) and it was possible that wind gusts at the outdoor air intake louvers might affect airflow patterns at the measurement section.

The flow grid that we constructed consisted of a wooden box fitted around the return damper assembly, with a set of five tubes having three equally spaced small holes facing into the airflow and another set of five tubes downstream having similarly located and sized holes facing away from the airflow. Each upstream hole was drilled into a dimple that we hammered into the grid tube; this dimpling reduces the angular sensitivity of aligning the holes with the airflow. No dimpling was used on the downstream holes because they are less sensitive to the airflow approach angle. We used downstream holes rather than measuring the static pressure in the flow grid section so that we could obtain larger pressure difference signals. For each airflow direction, the 15 holes in the five tubes are manifolded together and therefore linearly “averaged”. Each supply fan had two such devices placed over the two adjacent sets of return air damper assemblies. Equal length tubing was used to manifold and therefore average the pressures from the corresponding sections of the two return grids. Figure II-4 shows one of the return flow grids installed on the top of an air-handler mixing box (the right hand damper assembly, at the edge of the picture, had not yet received its flow grid).



Figure II-4. An installed return flow grid assembly.

We calibrated the return flow grid by closing and sealing the outdoor air dampers. In this configuration, all the supply air flowed through the return flow grid. With the supply fan operating at various speeds, we monitored the pressure differences across the return and supply grids. Then, we calculated the supply airflow using the correlations described in the previous section and developed a correlation between the resulting airflow and the monitored return grid pressure difference data. We also collected data at several different return damper positions to confirm that there was no influence on the calibration for different damper positions. Figure II-5 shows a typical calibration result.

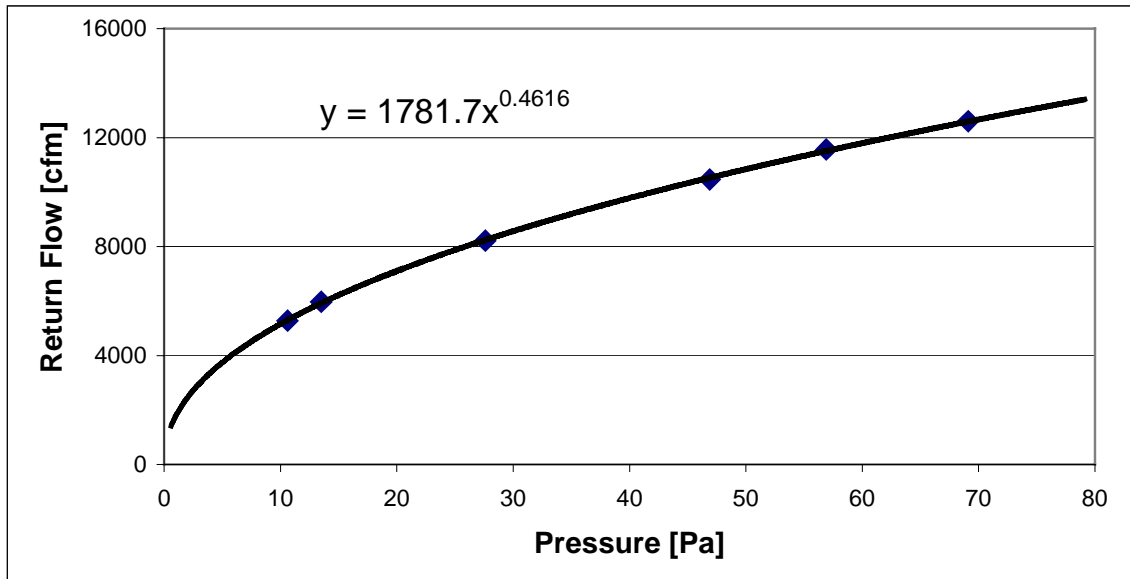


Figure II-5. Typical return flow grid calibration.

Calculation of Outdoor Airflow: The calculation of total outdoor airflow is simply the difference between the total supply airflow and the return airflow.

Calibration of VAV Box Primary Airflow Grids: Each VAV box has a factory installed radial flow grid. The EMCS monitors the primary airflow entering each VAV box using this grid and an adjacent pressure sensor. However, these flow grids and pressure sensors were apparently not calibrated in the installed configuration. This was evident in cases when the EMCS values indicated airflow when the air-handler supply fan was off. We confirmed this problem by turning the air-handler supply fans off and manually closing the primary air damper for the VAV box. For the four VAV boxes that we monitored in detail, we calibrated these flow grids using the same tracer gas method that we used to calibrate the air-handler supply fan flow grids.

Calibration of Detailed VAV Induction Fan Airflows: The induction fans in the powered VAV boxes have gravity dampers at their outlet into the boxes. During testing and balancing, the maximum opening of these dampers can be adjusted to “fine tune” the induction fan airflow after coarse adjustments are made using fan motor speed taps. We found that many of these dampers were set at more than 50% closed. In addition, VAV box pressures (which create a backpressure for the induction fan) change as the primary airflow changes. Therefore, it is unlikely the induction fans could operate at their rated airflow. To determine these airflows, we measured the airflows directly using a calibrated fan and flow meter device (similar to the device used to measure supply grille airflows). We found that the fans have a nearly constant airflow regardless of the primary inlet airflow. It was not possible to use the tracer gas method to calibrate these airflows, because there was no practical way to fully mix the injected tracer gas before the ducts split off from the plenum downstream of the VAV box.

Determining Duct Leakage Airflows and Adding Additional Leakage

We determined the existing leakage airflows at a reference condition. This measurement involved measuring the airflow out of each supply grille during a fixed and known supply fan

airflow, and comparing the sum of the grille airflows to the supply fan airflow; the difference is the leakage. We also estimated the distribution of “base case” (pre-intervention) duct leakage airflows by correlating duct leakage area with observed pressure differences across the duct system walls. To determine the leakage areas, we used fan pressurization techniques on the upstream duct section and on a sample of six downstream sections to measure leakage area. Pressure differences were monitored using pressure taps and sensors that we installed.

As discussed later in the “Results of HVAC System Airflow Tests” section, the total “base case” leakage airflow of the intervention floor was low. Consequently, rather than sealing a leaky duct system to determine energy savings associated with duct leakage (as we originally intended), we instead added duct leaks in both the upstream section and downstream sections to test the hypothesis that duct leakage will lead to increased fan power.

“Base Case” Upstream Leakage: We estimated the “base case” duct leakage airflows upstream of the VAV boxes on the intervention floor by using a duct pressurization test. Although this test is a poor indicator of leakage airflow for duct sections where pressure differences are highly variable (the test only determines leakage area), we were able confirm that the pressure difference was essentially the same throughout the upstream section of the duct system. It is probable that this constant pressure assessment would not be true if only one of the two supply fans was used or if there was a very large difference between the VAV airflows on the East and West sides.

To carry out the duct pressurization test on the upstream duct section, we manually closed all 34 VAV box primary air dampers and sealed both air-handler supply fans at their inlets on the intervention floor. A panel with a calibrated fan and flow meter device was then installed in place of one supply fan access door. We monitored duct pressures at both supply fan plenums; these were essentially equal throughout the test. The resulting leakage curve includes the leakage of the VAV primary air dampers, which we estimated using laboratory measurements of one VAV box ($0.6 \text{ cm}^2 \text{ ELA}_{25}$ per damper). The upstream leakage is then the difference between the leakage curve we measured and the leakage curve of the leakage from all the VAV inlet dampers combined. The VAV inlet damper leakage was about 34% of the total measured upstream leakage.

Although the total leakage airflow, which includes primary air damper leakage, is well determined by this pressurization test ($\pm 5\%$ of leakage airflow, $< \pm 1\%$ of supply fan maximum airflow), it is difficult to estimate the error in the upstream leakage part with the dampers excluded, because we only measured the VAV inlet damper leakage of one unit.

“Base Case” Downstream Leakage: We estimated the total “base case” duct leakage airflows downstream of the VAV boxes from the difference between the total airflow supplied to the boxes and the sum of all the supply grille airflows. The total airflow supplied to the boxes is simply the difference between the fan airflow and the upstream leakage. To make these measurements, we needed a stable, reproducible system configuration. This configuration was to set all the VAV box dampers fully open (EMCS set to request 5,000 cfm for each VAV box, which is larger than the maximum airflow of any box), to fully close all the outdoor air dampers, to fully open the return dampers, to set the supply fans to maximum airflow, and to set the relief fans to off. We call this configuration the “sum of supplies” mode of operation.

To measure the supply grille airflows, we used our “powered flow hood”. Laboratory results (Walker et al. 2001, Wray et al. 2002) have shown this flow hood to be very accurate. However, it is also quite slow and cumbersome to use (it took five people 12 hours to measure the airflows from all 103 supply grilles).

Because this “sum of supplies” test was carried out over several nights, one supply grille was measured repeatedly in this configuration to check the system stability and repeatability. The airflow at this grille was repeatable to within $\pm 2\%$ for the various days that we set the system in this configuration. It should be noted that during one night of very high winds, the airflows varied widely and we were unable to use any results from that night. We found that repeatable measurements could be made when wind speeds were less than 15 mph.

To extrapolate this leakage from the “sum of supplies” mode to normal operation conditions, we assume that the downstream background leakage airflow is a constant fraction of the supply airflow delivered to the VAV boxes. Consequently, the “base case” downstream leakage at operating conditions is the fraction of background downstream leakage during the “sum of supplies” mode multiplied by the total airflow delivered to the VAV boxes at operating conditions.

Because of the difficulties in using our powered flow hood for this test, we also carried out field tests using five commercially available flow hoods to determine if they could be used to measure the grille airflows as accurately, but more rapidly. The tests were performed on four different multi-branch subsections of the VAV system, using one supply grille on each section (there were two to five grilles for any one subsection). We selected four grilles to cover a range of nominal grille airflows from 50 to 200 L/s (100 to 400 cfm). The grilles were all 2 ft square, 4-way throw, with a perforated face (3/16" holes, 1/4" on center). The VAV system was set in the “sum of supplies” mode as described in this section to provide constant airflow during the test period. On each grille, the five commercially available hoods were used in sequence to measure the airflows. The reference airflow for each grille was measured using our powered flow hood. Manufacturer's instructions for hood operation were followed in each case (e.g., the use of relief vents or low-flow plates). We found that it was essential to follow instructions properly because it was easy to use the wrong operating mode and get large errors (e.g., we found an error of 38% by using incorrect vent modes for one of the flow hoods).

The results of these field tests are summarized in Table II-3. The results show that the hoods exhibited similar trends, with under-prediction of low airflows. Overall, Flow Hood 1 had the best performance with bias and RMS errors less than 2%. This RMS difference is close to the accuracy of the powered flow hood itself, which shows that for this grille type, Flow Hood 1 can give the same results as our reference device within the uncertainty specification of the reference. Flow Hoods 3 and 5 were a little worse, with RMS errors approaching 5%. Flow Hoods 2 and 4 exhibited significant biases and under-predicted airflows by more than 10%.

Table II-3. Summary of field test results for five commercially available flow hoods on four commercial grilles.

Flow Hood	Bias Error, L/s (cfm)	Bias Error, %	RMS Error, L/s (cfm)	RMS Error, %
1	1 (3)	1	2 (4)	2
2	-14 (-29)	-11	17 (36)	11
3	6 (12)	4	7 (15)	5
4	-9 (-20)	-11	10 (21)	14
5	-3 (-7)	-2	6 (12)	4

Our tests indicated that 20 grille airflows could be measured in 35 minutes using Hood 1. This means that two people each using a hood could measure 100 grille airflows in less than two hours. Because hood accuracy depends on grille type, further work is needed to determine if these results can be extended to other buildings.

Installed Upstream Leaks: We installed duct leaks in the main duct loop upstream of the VAV boxes at five locations. The leaks consisted of a perforated plate (similar to the perforated plates that are used in the supply grilles), which we mounted in an end cap covered with cardboard. All these leaks were installed on ten inch diameter ducts that protruded out from the existing main loop by 1 to 3 feet. Figure II-6 shows one of these installed leaks.

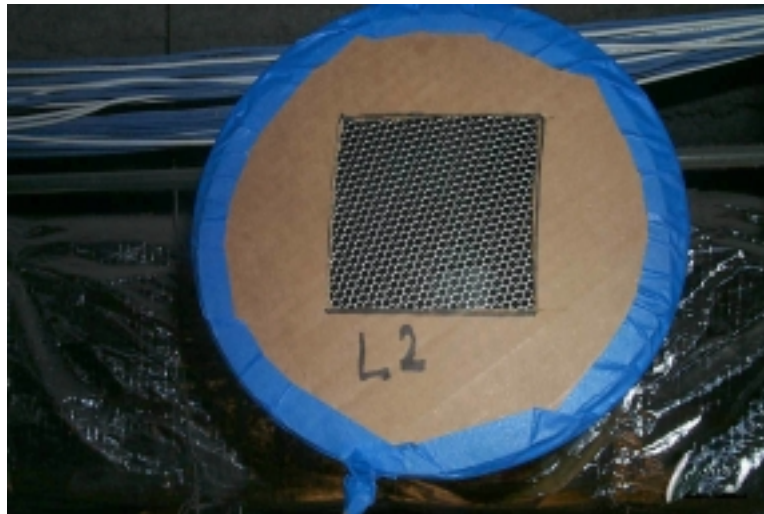


Figure II-6. Example of an installed upstream leak.

The amount of leakage was adjusted by cutting out a section of the cardboard. We had calibrated the perforated plate in the laboratory to determine its leakage characteristic per unit area. The pressure difference seen by the upstream leakage was found to be the same at all five leak sites over a wide range of total supply airflows, so we only needed to monitor one pressure difference to determine all the leakage airflows through the upstream leaks that we added.

Installed Downstream Leaks: We also installed leaks in six locations downstream of the VAV boxes. To determine which VAV boxes had enough capacity to accommodate the leakage airflows and still provide the design airflow to the occupants, we set each VAV box in turn to its

maximum airflow at “design static pressure” and recorded these airflows. The branches that we selected were from all four sides of the building and included both core and perimeter zones.

The installed downstream leaks used the same material as the installed upstream leaks. An example is shown in Figure II-7.

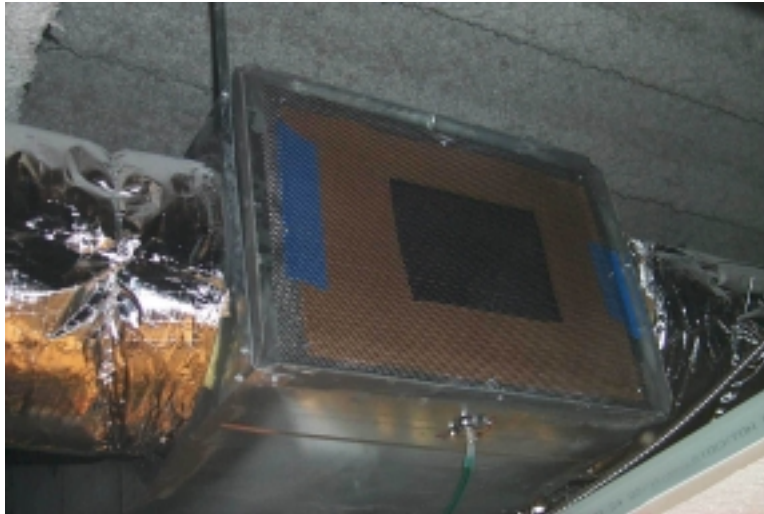


Figure II-7. Example of an installed downstream leak at the end of a plenum. Ducts can be seen exiting two sides of the plenum. A static pressure sensor is mounted adjacent to the installed leak.

A correlation between the pressure difference across each installed downstream leak and the corresponding upstream primary airflow was obtained by fitting curves to pressure differences that we measured during diagnostic tests at various VAV primary airflows (obtained from the EMCS), with and without the induction fan operating (if the box had a fan). A separate relationship was needed when induction fans were used, because the induction fans add airflow downstream of the VAV box primary airflow grids.

Analysis of Results

To evaluate the effects of upstream and downstream duct leakage separately and in combination, we monitored the performance of the intervention floor system over four test periods, defined as:

1. Base (pre-intervention conditions)
2. Upstream (leaks added to the main duct loop)
3. Downstream (leaks added to the ducts downstream of the VAV boxes)
4. Upstream and Downstream (leaks added to the loop and downstream of the VAV boxes)

For comparison, we conducted similar monitoring of the control floor during the same test periods. However, we made no changes to the ducts on that floor. The test periods ranged from one to two weeks each and took place during the summer of 2002. We looked at overall impacts (full day analysis – 3 am to 6 pm) as well as utility peak period impacts (2 pm to 6 pm). To

compare a variable for the same time period for both the control and intervention floor, we included only those observations when air-handler supply fans were operating on both the control and intervention floors.

Results of HVAC System Airflow Tests

Air-Handler Supply Airflows: Table II-4 lists the average supply fan airflows for the intervention floor during the various test periods, without corrections for weather differences.

Table II-4. Average supply fan airflow (cfm) during testing period (intervention floor, not weather corrected).

Operating Period	Leakage Configuration			
	“Base”	“Up”	“Down”	“Up & Down”
All Day	10,700	11,900	12,800	14,100
Peak Hours	11,300	11,900	12,000	13,900

*All day refers to the 3 am to 6 pm period while peak refers to the 2 pm to 6 pm period.

As Figure II-8 shows, daily average air-handler supply fan airflows for the control (16th) and intervention (17th) floors varied in response to weather-induced thermal loads driven by the outdoor air temperature. In particular, these airflows generally increased over the entire measurement period, with larger airflows occurring in the hotter months. For all seasons, the airflows for the control (16th) floor were larger than the airflows for the intervention (17th) floor.

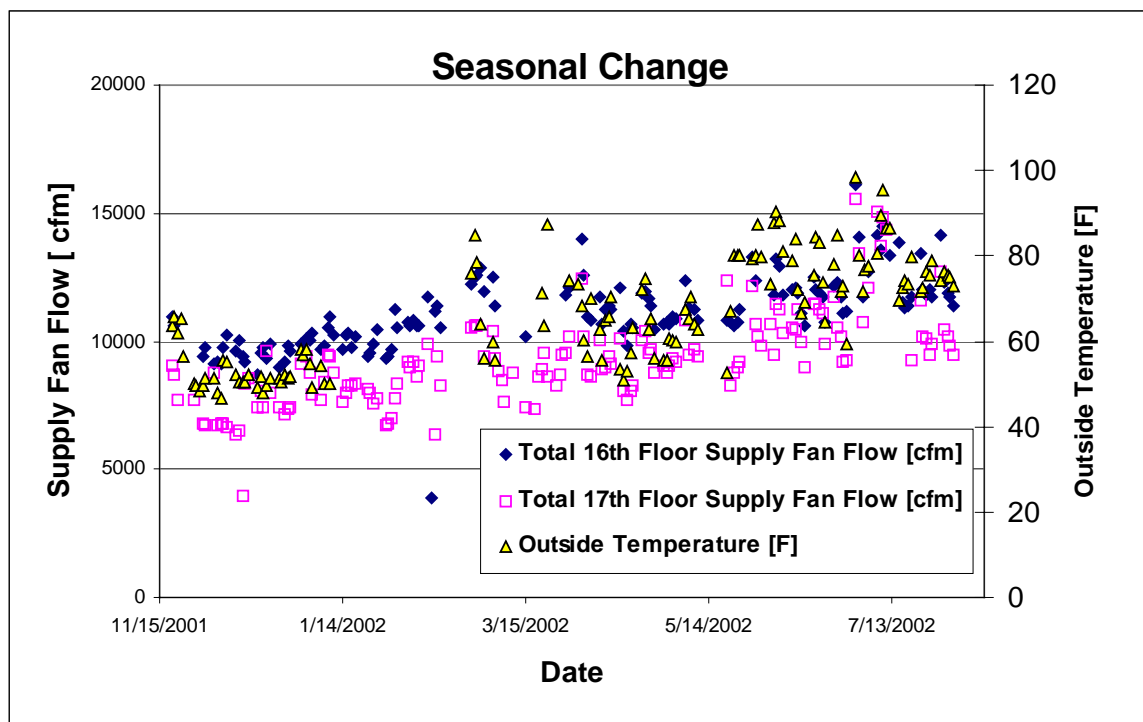


Figure II-8. Daily average supply fan airflow and outdoor temperature for the entire measurement period.

Although the four leakage intervention study periods took place during the summer of 2002 with similar occupancy patterns on both floors, the weather conditions during each period were somewhat different from each other. Table II-5 lists the average outdoor temperatures for each test period, as recorded by the EMCS.

Table II-5. Average outdoor temperature (°F).

Leakage Configuration	All Day (3 am to 6 pm)	Peak Period (2 pm to 6 pm)
Base	77	90
Up	78	80
Down	81	93
Up & Down	89	102

It is important to note that the supply airflows exiting the air-handlers during operating periods were not constant, even over the course of a day. Figure II-9 shows an example of the daily behavior of air-handler supply airflows for the “Base Case” condition.

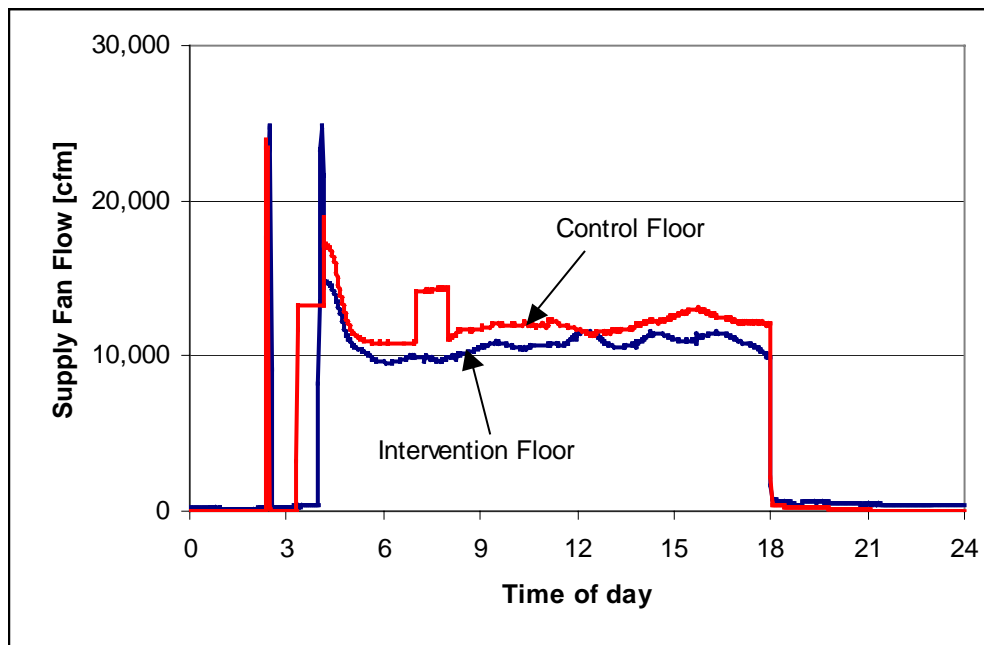


Figure II-9. Supply fan airflows from a sample “Base Case” day.

Figure II-9 shows a number of interesting features:

- At about 2:30 a.m. every day, the fans are turned on for a five minute long “system check”.
- On the example day shown (July 23, 2002), one of the supply fans on the control floor is turned on at about 3:30 a.m. for about half an hour to precool the floor.
- The abrupt increase in the control floor supply airflows at about 7 a.m. is typical behavior during the summertime evaluation period. It is not know why this increase occurs.

- Generally ,the supply airflows are larger than average during the first hours of “normal” operation starting at 4 a.m.
- The HVAC system is turned off at 6 p.m. every day.

Weather Normalization: To take the temperature differences and corresponding operational differences into account for different periods, a normalization procedure can be used to compare the airflows (or other variable such as power) measured during the leakage case test periods to that measured during the base case period. The fractional change in value is calculated as follows:

$$Fractional \cdot Change = \frac{\overline{X}_{IL} - \overline{X}_{IB}}{\overline{X}_{IB}} * \frac{\overline{X}_{CB}}{\overline{X}_{CL}} \quad (2)$$

where:

- X = the variable being studied for the time period specified,
- IL = intervention floor, leakage case time period,
- IB = intervention floor, base case time period,
- CL = control floor, leakage case time period, and
- CB = control floor, base case time period.

The first part of Equation 2, based on the intervention floor data, calculates the intervention floor fractional change in a value due to the additional duct leakage installed. The second part of Equation 2 provides a normalization factor using the control floor data. The result is the fractional change in the variable studied (e.g., airflows, power, induction fan on-time).

This equation can be further derived to estimate what the airflows (or other variable) would be if the intervention floor was operated in a given leakage case mode during the base period. The derivation of this equation is:

$$\overline{X}_{IBL} = \overline{X}_{IB} * (1 + Fractional \cdot Change * (\overline{X}_{CL} / \overline{X}_{CB})) \quad (3)$$

where:

- \overline{X}_{IBL} = Estimate of what the variable average value would be if the corresponding case took place during the base case time period.

Unless otherwise noted, these equations were used to calculate the normalized changes due to duct leakage for the two time segments (all day and peak). In order to compare a variable for the same time period for both the control and intervention floor, we included only those observations when both control and intervention floor air-handler supply fans were on.

Using these normalization techniques for each leakage case, we have estimated what the average air-handler supply airflow would be if we ran the system in a given leakage case, but during the base case weather period instead. As shown in Table II-6, the base case average airflows range from 10,700 cfm (all day) to 11,300 cfm (peak). If the system were to operate in a leakage case over the same time period, we estimate these values would range from 11,900 (all day and peak) to 13,400 (all day) and to 13,600 (peak). Due to higher supply fan airflows during the morning cool-down period, the all day average impacts are greater than that found for the peak period. In

both all day and peak period analyses, the impact of the downstream leakage case (18% all day and 7% peak) is greater than that of the upstream leakage case (11% all day and 6% peak). The greatest impact is when there are both upstream and downstream leaks (28% all day and 22% peak period).

Table II-6. Normalized average airflow (cfm) for air-handler supply fans.

Leakage Configuration	% Change in Airflow		Estimated Average Airflow for Base Case Test Period (cfm)	
	All Day (3 am to 6 pm)	Peak (2 pm to 6 pm)	All Day (3 am to 6 pm)	Peak (2 pm to 6 pm)
Base	-	-	10,700*	11,300*
Up	11%	6%	11,900	11,900
Down	18%	7%	12,400	12,000
Up & Down	28%	22%	13,400	13,600

*base case averages.

VAV Box Primary Airflows: Most VAV primary air inlet airflows quickly settled down to nearly constant values for the day. The exception being the behavior of VAV Box 1712 (fan powered). Figure II-10 shows a sample “Base” day of the VAV box primary airflows for the four boxes that we monitored in detail.

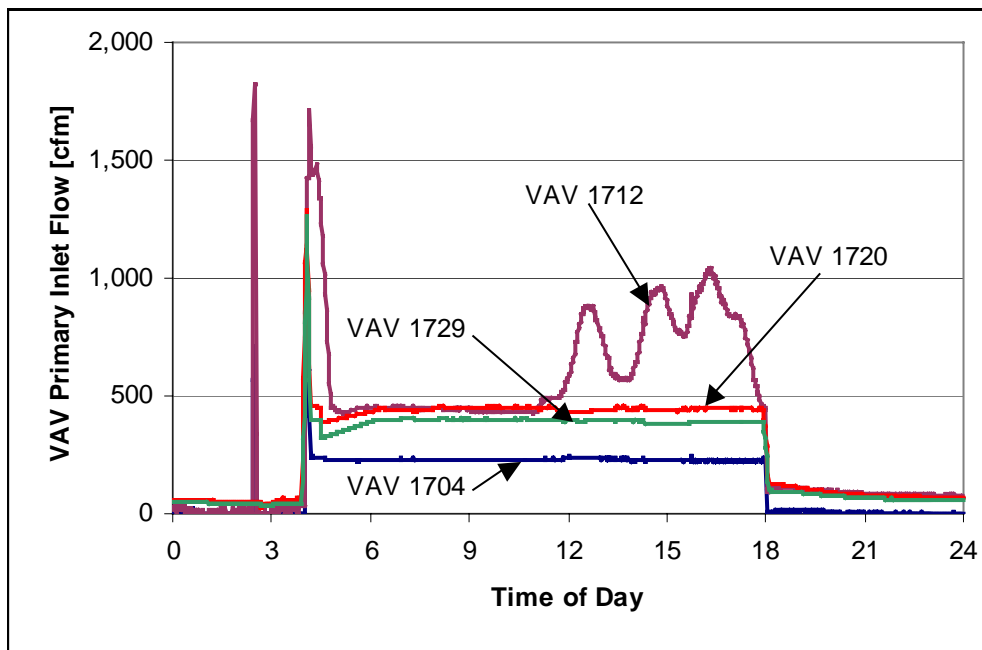


Figure II-10. Four selected VAV box primary airflows for a sample “Base Case” day.

Duct Leakage Airflows at Operating Conditions: Table II-7 lists the average upstream, downstream, and total leakage fractions and airflows during the various leakage configurations.

Table II-7. Average upstream, downstream, and total leakage fractions and leakage airflows.

Operating Period	Leak Location	Leakage Configuration							
		“Base”		“Up”		“Down”		“Up & Down”	
		Leakage (%)	Flow (cfm)	Leakage (%)	Flow (cfm)	Leakage (%)	Flow (cfm)	Leakage (%)	Flow (cfm)
All Day	Upstream	3.2	340	14.6	1,737	2.7	340	12.3	1,738
	Downstream	2.3	245	2.0	239	8.0	1,022	7.4	1,042
	Total	5.5	585	16.6	1,976	10.7	1,362	19.7	2,780
Peak Hours	Upstream	3.0	340	14.6	1,737	2.8	340	12.5	1,737
	Downstream	2.3	258	2.0	239	8.3	990	7.4	1,022
	Total	5.3	598	16.6	1,976	11.1	1,330	19.9	2,759

The leakage fractions in Table II-7 are determined as a percentage of the total supply fan airflow measured during the corresponding operation and leak configuration period (not weather corrected). Note that the leakage fraction of the “Up & Down” case is not the sum of the “Up” and the “Down” case, because the background leakage would be counted twice and because the total supply fan airflow changes for each case. However, upstream and downstream leakage fractions combine directly in any particular case and equal the total leakage fraction in that case.

Figure II-11 shows how the duct leakage airflows vary over a sample day for the “Up & Down” configuration.

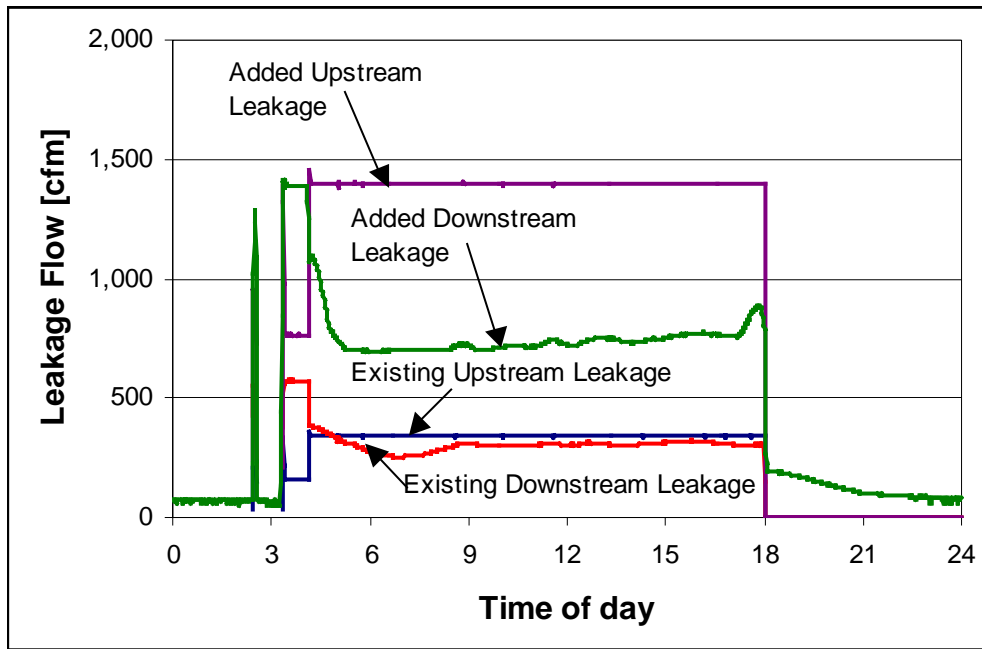


Figure II-11. Duct leakage airflows for a sample “Up & Down” day.

Regardless of the leakage configuration and supply fan airflow, the upstream leaks are at an almost constant pressure (the “design static pressure”) and therefore have a nearly constant

leakage airflow throughout the “normal operating” hours. This is a result of the system design: the pressure in the main duct where the upstream leaks are located is controlled to maintain the “design” set point of 1 in. w.c. (250 Pa). In contrast, the downstream leakage airflow varies as each of the six VAV boxes that had leaks installed vary their primary airflow and as induction fans start and stop.

Duct Leakage Airflows at “Design” Conditions: The duct leakage airflows discussed in the previous section are the actual values found during our measurement period. If one wants to specify a leakage requirement for a performance standard, then the system configuration will need to be specified.

We define the leakage performance standard conditions to be:

- The air-handler supply fan should be at 100% of its full rated speed.
- The air-handler supply fan airflow shall maintain the maximum designed static pressure.
- The VAV boxes are uniformly open (all are at the same fraction of their design maximum airflow) to the maximum degree possible while the first two conditions are met.
- All induction fans, terminal heaters, and relief fans are off.
- The return dampers are fully open and the outdoor air dampers are closed as much as possible.

These conditions apply to the type of control system that was used in our test building. There may be additional specifications needed for other system layouts and controls.

In our test building, we produced these conditions during the “Base Case” test period by adjusting the VAV primary airflow set points until we were just able to maintain the design static pressure of 1 in. w.c. (250 Pa). This operating point corresponds to the VAV boxes being set at 75% of their “cooling maximum” airflows and the total supply fan airflow at 24,400 cfm. We call this airflow the “design static airflow”.

In Table II-8 for each of the leakage configurations, we list the upstream, downstream, and total duct leakage airflows themselves, and as a fraction of the “design static airflow”. Note that the system never operated in this leakage performance configuration.

Table II-8. Leakage airflows and leakage fraction of supply fan airflow at the “design static airflow” of 24,400 cfm.

		Leakage Configuration							
		“Base”		“Up”		“Down”		“Up & Down”	
Operating Period	Leak Location	Leakage (%)	Flow (cfm)	Leakage (%)	Flow (cfm)	Leakage (%)	Flow (cfm)	Leakage (%)	Flow (cfm)
“Design”	Upstream	1.4	340	7.1	1,737	1.4	340	7.1	1,737
	Downstream	2.3	567	2.2	534	6.5	1,595	6.2	1,507
	Total	3.7	907	9.3	2,271	7.9	1,935	13.3	3,244

Economizer Operation: An economizer can be used to mix outdoor air with return air to reduce cooling coil loads when the enthalpy of the outdoor air is lower than the enthalpy of the return

air. The economizer mode can also be used to precool the building; building engineering staff advised us that the EMCS has been configured to enable economizer operation for precooling based on an EMCS survey of temperatures at midnight. During the summer evaluation period, the economizer was often used for precooling, but there was no consistency between usage on the control and intervention floors. In particular, the time that the control floor economizer would start operating varied from day to day; the economizer on the intervention floor sometimes started at a different time, or not at all. This suggests that the economizer may have been regulated by means other than the stated EMCS control sequence, such as an optimal start routine.

The daily variation in outdoor airflows entering the supply fan is complex, as shown in Figure II-12. This figure shows airflows for the West side of the control floor. The supply airflow is mostly composed of outdoor air with some abrupt drops in total outdoor airflow and corresponding abrupt increases in the minimum outdoor airflow. These changes can happen at any time during the normal occupied hours. Also interesting is the time from about 3 to 4 a.m. when the East side fan is on for precooling. In these conditions, the East fan pressurizes all of the duct system, including the West side air-handler, resulting in airflow going out of the West outdoor air intake.

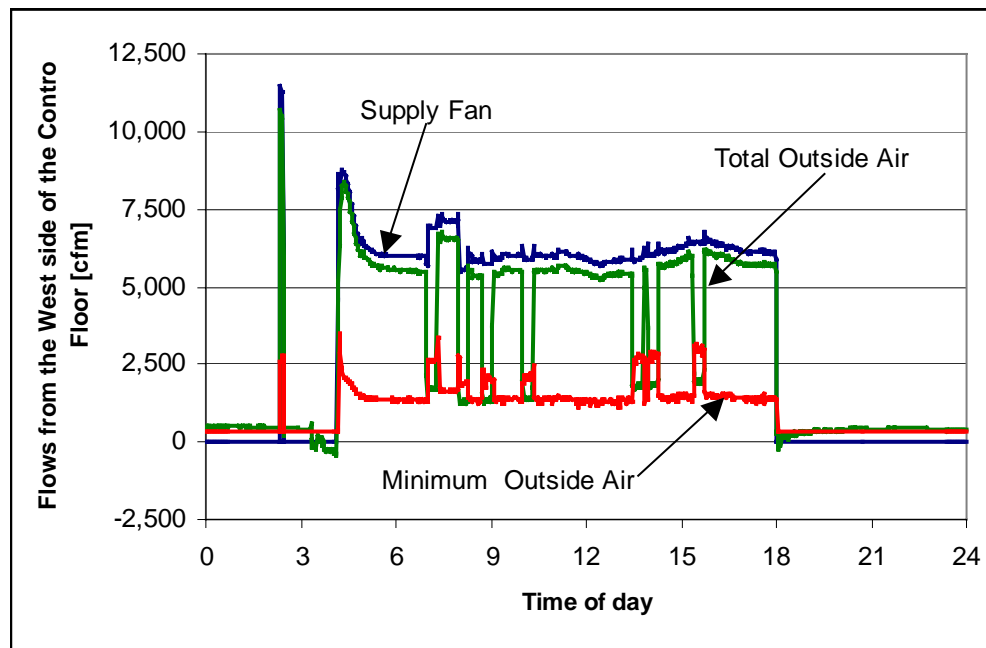


Figure II-12. West supply fan and outdoor airflows on the control floor, for a sample “Base Case” day.

The fluctuating behavior of the economizer operation makes it difficult to compare economizer behavior for the different leakage cases. One would expect that supply air leaking into the return air would cool that air and therefore return air would be selected over outdoor air (less economizer usage). While our data in Table II-9 seems to support this behavior on the intervention floor, most notably for the “Up & Down” case, we feel that result is not well characterized, particularly because the outdoor air temperature during the “Up & Down” case

was much higher than the other cases. This influence can be seen in the variation of the outdoor air fractions for the control floor during the different leakage cases.

Table II-9. Average outdoor air fraction of supply airflow.

Operating Period	Leakage Configuration							
	“Base”		“Up”		“Down”		“Up & Down”	
	Control Floor	Intervention Floor	Control Floor	Intervention Floor	Control Floor	Intervention Floor	Control Floor	Intervention Floor
All Day	66%	38%	58%	35%	60%	35%	32%	29%
Peak Hours	44%	48%	46%	45%	35%	44%	20%	32%

Fan Power Impacts of Duct Leakage

A significant objective of this project is to determine whether the presence of duct leakage changes the amount of electricity required to operate the distribution system fans. We studied this by measuring and calculating fan power during the four test periods. For comparison, we measured and calculated fan power for the control floor during the same test periods.

Fan Power due to Increased Duct Leakage: During the cooling season, the amount of electrical power required by the HVAC system to transport conditioned air includes the power to drive the air-handler supply fans, relief fans, and VAV box induction fans. In reviewing the patterns of fan operation, we found that the supply fan and induction fan airflows and operation are impacted by the introduction of additional duct leakage. The relief fans are operated to maintain building pressure set points and run as needed during pre-cooling and economizer modes. As a result the relief fans have an irregular operational pattern. We did not see a correlation between duct leakage and relief fan operation. As such, we will only discuss the impact of duct leakage on the air-handler supply fans and the induction fans, and not on the relief fans.

Air-Handler Fan Power: Table II-10 summarizes the increase in air-handler supply fan power for each of the leakage cases compared to the base case.

Table II-10. Normalized average fan power (kW) for air-handler supply fans.

Case	% Change in Fan Power for Air-Handler Supply Fans		Estimated Average Fan Power for Air-Handler Supply Fans for Base Case Test Period (kW)	
	All Day (3 am to 6 pm)	Peak (2 pm to 6 pm)	All Day (3 am to 6 pm)	Peak (2 pm to 6 pm)
Base	-	-	5.4*	5.8*
Up	16%	10%	6.2	6.4
Down	26%	11%	6.5	6.4
Up & Down	37%	28%	7.0	7.2

*base case averages.

The increase in air-handler supply fan power is driven by the increased airflow required to meet thermal conditions for a given leakage case. Following the trend of the weather-corrected

changes in supply airflow required (Table II-6), the greatest increase in fan power is for the upstream and downstream leakage case (37% all day and 28% peak). The downstream leakage case (26% all day and 11% peak) requires a greater increase in fan power than the upstream leakage case (16% all day and 10% peak). The base case average fan power ranges from 5.4 (all day) to 5.8 kW (peak). If the system were to operate in the leakage cases over the same time period, we estimate that the average fan power would range from 6.2 to 7.0 kW (all day) and from 6.4 to 7.2 kW (peak).

Induction Fan Power: The EMCS adjusts the amount of air delivered to a given zone via the VAV box’s primary air damper, based on the zone temperature reading and throttling range set point. If the amount of primary airflow entering the VAV box is lower than a specified threshold, in this case less than 40% of the box’s cooling maximum airflow, the EMCS turns on the induction fan in the VAV box. The induction fan pulls air from the ceiling plenum (return plenum) into the VAV box.

Table II-11 summarizes, on average, the fraction of induction fans operating during each test period. When there is a higher amount of downstream leakage, the powered VAV boxes operate at higher primary airflows to compensate for the leakage and the induction fans do not run as often. This decrease in induction fan on-time contributes to lower induction fan power required to meet thermal conditions.

Table II-11. Normalized average fraction of induction fans operating.

Case	% Change in Fraction of Induction Fans Operating		Estimated Average Fraction of Induction Fans Operating for Base Case Test Period	
	All Day (3 am to 6 pm)	Peak (2 pm to 6 pm)	All Day (3 am to 6 pm)	Peak (2 pm to 6 pm)
Base	-	-	0.72*	0.63*
Up	0%	3%	0.72	0.65
Down	-37%	-23%	0.40	0.48
Up & Down	-43%	-36%	0.29	0.34

*base case averages.

On average during the base case, the induction fans were running 72% (all day) and 63% (peak). If we were to operate the system in the leakage cases over the base case time period, we estimate that the percentage of induction fans running would increase slightly for the upstream case (72% all day and 65% peak), but decrease for the downstream case (40% all day and 48% peak) and the upstream and downstream case (29% all day and 34% peak).

The induction fans (on average, 1.3 kW all day and 1.2 kW peak for the base case) use about one-fifth as much fan power as the air-handler supply fans. The reduction in the fraction of induction fans operating translates directly into lower induction fan power needed to meet the thermal requirements of each leakage case (see Table II-12). The downstream case requires 38% (all day) and 24% (peak) less induction fan power and the upstream and downstream case requires 45% (all day) and 38% (peak) less induction fan power than the base case. For the base case period, this reduces the induction fan power to an estimated 0.7 kW (all day) and 0.9 kW (peak) for the downstream case and an estimated 0.5 kW (all day) and 0.6 kW (peak) for the upstream and downstream case.

Table II-12. Normalized average fan power (kW) for induction fans.

Case	% Change in Induction Fan Power		Estimated Average Induction Fan Power for Base Case Test Period (kW)	
	All Day (3 am to 6 pm)	Peak (2 pm to 6 pm)	All Day (3 am to 6 pm)	Peak (2 pm to 6 pm)
Base	-	-	1.3*	1.2*
Up	0%	3%	1.3	1.2
Down	-38%	-24%	0.7	0.9
Up & Down	-45%	-38%	0.5	0.6

*base case averages.

Air-Handler Supply and Induction Fan Power: The increases in air-handler supply fan power, seen in Table II-10, are tempered by the decrease in induction fan power, seen in Table II-12, resulting in a net increase in air-handler supply and induction fan total power of 13% (all day) and 9% (peak) for the upstream case, 17% (all day) and 6% (peak) for the downstream case, and 26% (all day) and 19% (peak) for the upstream and downstream case (see Table II-13).

Table II-13. Normalized average fan power (kW) for air-handler supply and induction fans.**

Case	% Change in Air-Handler Supply and Induction Fan Power		Estimated Average Air-Handler Supply Fan and Induction Fan Power for Base Case Test Period (kW)	
	All Day (3 am to 6 pm)	Peak (2 pm to 6 pm)	All Day (3 am to 6 pm)	Peak (2 pm to 6 pm)
Base	-	-	6.7*	6.9*
Up	13%	9%	7.6	7.6
Down	17%	6%	7.7	7.3
Up & Down	26%	19%	8.3	8.2

*base case averages.

**Because the total supply and induction fan power values are the averages based on the sum of the coincident fan power measurements, the sum of the average individual supply and induction fan power may not add to be the average total supply and induction fan power results.

For the base case, the net average air-handler supply fan and induction fan total power is 6.7 kW (all day) and 6.9 kW (peak). We estimate that, by operating the leakage cases in the base case time period, the net average air-handler supply fan and induction fan total power would increase to 7.6 kW (all day or peak) for the upstream case, 7.7 kW (all day) and 7.6 kW (peak) for the downstream case, and 8.3 (all day) and 8.2 (peak) for the upstream and downstream case.

Fan Power Metrics: As described in Appendix I, there are several metrics that can be used to characterize the performance of thermal distribution systems. We have focused here on those related to system fan power. These include specific fan power (W/cfm), normalized fan power (W/ft²), and fan-airflow density (cfm/ft²).

Specific Fan Power (W/cfm): The specific fan power (W/cfm) is calculated, for constant volume systems, as the total fan power divided by the total delivered airflow at the supply grilles. This metric accounts for the fan power only and does not reflect any thermal losses in the duct system.

As such, it quantifies the amount of fan power required to deliver a given quantity of air through the duct system to the space or building. This parameter is relatively constant in a constant-air-volume system, because the fan speed and the airflow to the grilles remain constant for a given operating state (heating, cooling, or ventilation).

This is not true for the test building, which has a variable-air-volume system with variable frequency drive fans and powered induction boxes. In this system, the amount of air delivered to each grille and the amount of power required to drive the supply, relief, and induction fans can vary widely throughout the day depending on zone conditioning load requirements. Although we have measured air-handler supply and induction fan power on a minute by minute basis, measuring the airflow delivered to each grille on the same basis would require a level of airflow monitoring that is beyond the scope of this project. Instead, we calculated the specific air-handler fan power value as the power for the air-handler supply fans divided by the airflow through the air-handler supply fans (See Table II-14). This parameter can be used to compare air-handler fan power for our various leakage cases.

Table II-14. Specific fan power (W/cfm) for air-handler supply fans.**

Case	% Change in Specific Fan Power		Estimated Specific Fan Power for Base Case Test Period (W_{fan}/cfm)	
	All Day (3 am to 6 pm)	Peak (2 pm to 6 pm)	All Day (3 am to 6 pm)	Peak (2 pm to 6 pm)
Base	-	-	0.50*	0.51*
Up	4%	4%	0.52	0.53
Down	7%	5%	0.53	0.53
Up & Down	9%	6%	0.54	0.54

*base case averages.

**based on airflows through the air-handler supply fans and not the airflows at the grilles.

Because the air-handler supply fan power increases as the air-handler supply fan airflow increases, the changes in specific fan power for the air-handler supply fan are relatively low, increasing 4% (all day or peak) for the upstream case, 7% (all day) and 5% (peak) for the downstream case, and 9% (all day) and 6% (peak) for the upstream and downstream case.

For the base case, the specific fan power is 0.50 W/cfm (all day) and 0.51 W/cfm (peak). The specific fan power increases slightly to range from 0.52 to 0.54 W/cfm for the leakage cases.

Normalized Fan Power (W/ft^2): This metric reflects the impacts of duct leaks and thermal losses and is primarily used as a metric for constant volume systems. For the purpose of this building with a VAV system, we have evaluated this metric based on how it was operated during our test periods.

Based on the operation of the building during our test periods, Tables II-15 through II-17 summarize normalized fan power for the air-handler supply fans, the induction fans, and the net supply and induction fan totals. The base case normalized fan power is 0.18 W/ft^2 (all day) and 0.20 W/ft^2 (peak) for the air-handler supply fan, 0.05 W/ft^2 (all day) and 0.04 W/ft^2 (peak) for the induction fans, and 0.23 W/ft^2 (all day) and 0.24 W/ft^2 (peak) for the net total of the air-handler supply and induction fans. These values change in the same way as the fractional changes for the fan powers (Tables II-10, II-12, and II-13) and the estimated values range from 0.21 to 0.25 W/ft^2

for the air-handler fans, 0.02 to 0.05 W/ft² for the induction fans, and 0.25 to 0.29 W/ft² for the net total air-handler supply and induction fans.

Table II-15. Normalized fan power (W/ft²) for air-handler supply fans.

Case	% Change in Normalized Fan Power for Air-Handler Supply Fans		Estimated Normalized Fan Power for Air-Handler Supply Fans for Base Case Test Period (W/ft ²)	
	All Day (3 am to 6 pm)	Peak (2 pm to 6 pm)	All Day (3 am to 6 pm)	Peak (2 pm to 6 pm)
Base	-	-	0.18*	0.20*
Up	16%	10%	0.21	0.22
Down	26%	11%	0.22	0.22
Up & Down	37%	28%	0.24	0.25

*base case averages.

Table II-16. Normalized fan power (W/ft²) for induction fans.

Case	% Change in Normalized Fan Power for Induction Fans		Estimated Normalized Fan Power for Induction Fans for Base Case Test Period (W/ft ²)	
	All Day (3 am to 6 pm)	Peak (2 pm to 6 pm)	All Day (3 am to 6 pm)	Peak (2 pm to 6 pm)
Base	-	-	0.05*	0.04*
Up	0%	3%	0.05	0.04
Down	-38%	-24%	0.02	0.03
Up & Down	-45%	-38%	0.02	0.02

*base case averages.

Table II-17. Normalized fan power (W/ft²) for air-handler supply and induction fans.

Case	% Change in Normalized Fan Power for Air-Handler Supply Fans and Induction Fans		Estimated Normalized Fan Power (Air-Handler Supply Fans and Induction Fans for Base Case Test Period (W/ft ²))	
	All Day (3 am to 6 pm)	Peak (2 pm to 6 pm)	All Day (3 am to 6 pm)	Peak (2 pm to 6 pm)
Base	-	-	0.23*	0.24*
Up	12%	9%	0.26	0.26
Down	17%	6%	0.26	0.25
Up & Down	26%	19%	0.29	0.28

*base case averages.

Fan-Airflow Density (cfm/ft²): For a constant-air-volume system, the fan-airflow density metric (cfm/ft²) can be determined by measuring the floor area and the total airflow delivered to each zone under certain operating conditions and by calculating the airflow per unit floor area in each zone. This metric reflects the impacts of thermal losses while not discounting duct leakage in a significant way.

For a VAV system, the amount of monitoring required to calculate this metric during occupied hours would be excessive. Rather than report an artificial value calculated by setting the system into a constant volume mode, we have redefined the fan-airflow density metric here to be the airflow measured at the air-handler supply fans divided by the floor area. As can be seen in Table II-18, this value is affected by the amount of duct leakage seen by the system and increases at the same rate as the air-handler supply fan airflows listed in Table II-6: 11% (all day) and 6% (peak) for the upstream case; 18% (all day) and 7% (peak) for the downstream case; and 28% (all day) and 22% (peak) for the upstream and downstream case.

Table II-18. Fan-airflow density (cfm/ft²) for air-handler supply fans.

Case	% Change in Fan-Airflow Density for Air-Handler Supply Fans		Estimated Fan-Airflow Density for Air-Handler Supply Fans for Base Case Test Period (cfm/ft ²)	
	All Day (3 am to 6 pm)	Peak (2 pm to 6 pm)	All Day (3 am to 6 pm)	Peak (2 pm to 6 pm)
Base	-	-	0.37*	0.39*
Up	11%	6%	0.41	0.41
Down	18%	7%	0.43	0.41
Up & Down	28%	22%	0.46	0.47

*base case averages.

For the base case, the fan-airflow density is 0.37 cfm/ft² (all day) and 0.39 cfm/ft² (peak). Our estimates for the leakage cases operating during the base case range from 0.41 cfm/ft² (all day and peak) for the upstream case, 0.43 cfm/ft² (all day) and 0.41 cfm/ft² (peak) for the downstream case, and 0.46 cfm/ft² (all day) and 0.47 cfm/ft² (peak) for the upstream and downstream case.

Zone Air Temperatures: The presence of additional duct leakage did not change the average zone air temperatures significantly, as determined by the thermostat data obtained using the EMCS (see Table II-19). Looking at the six zones in which we added duct leakage downstream of the VAV boxes, we found that temperatures remained within 0.1°F between cases and well within thermal comfort requirements. This is due to the additional fan power available to move conditioned air to meet the comfort requirements of the space.

Table II-19. Normalized average zone air temperatures (°F).

Case	Estimated Average Zone Temperature for Base Case Test Period (°F)	
	All Day (3 am to 6 pm)	Peak (2 pm to 6 pm)
Base	73.9*	73.9*
Up	73.8	73.8
Down	73.9	73.8
Up & Down	73.9	73.8

*base case averages.

Fan Power Trends: Figures II-13 and II-14 show general daily fan power trends using two sample days: a “Base Case” day (no added duct leaks) and an “Up & Down” day (with upstream and downstream duct leaks installed). Note that one might consider assessing duct leakage effects on fan power by simply comparing the daily fan power trends for the two cases. This approach does not account for occupancy and weather differences between cases.

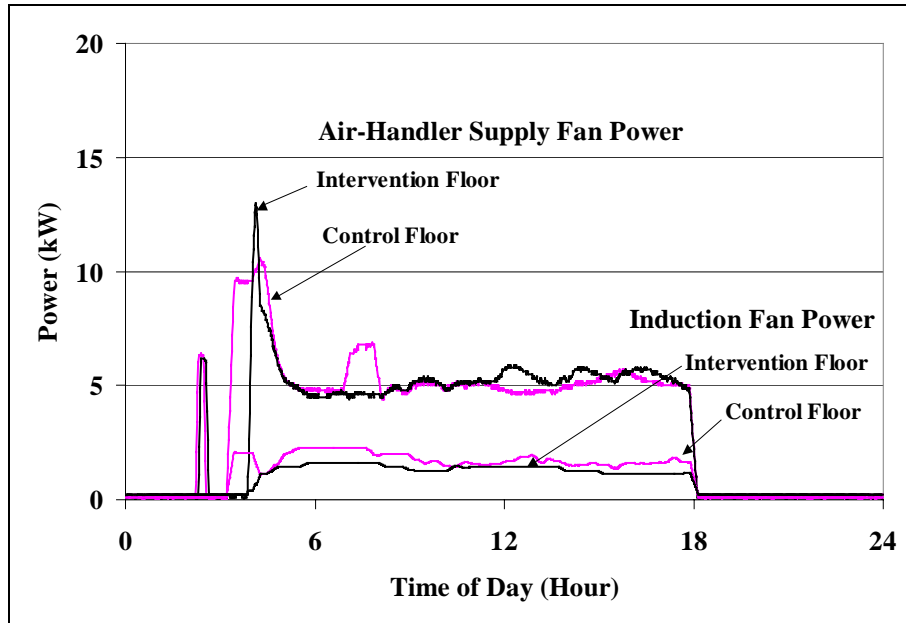


Figure II-13. Air-handler supply fan and induction fan power for a sample “Base Case” day.

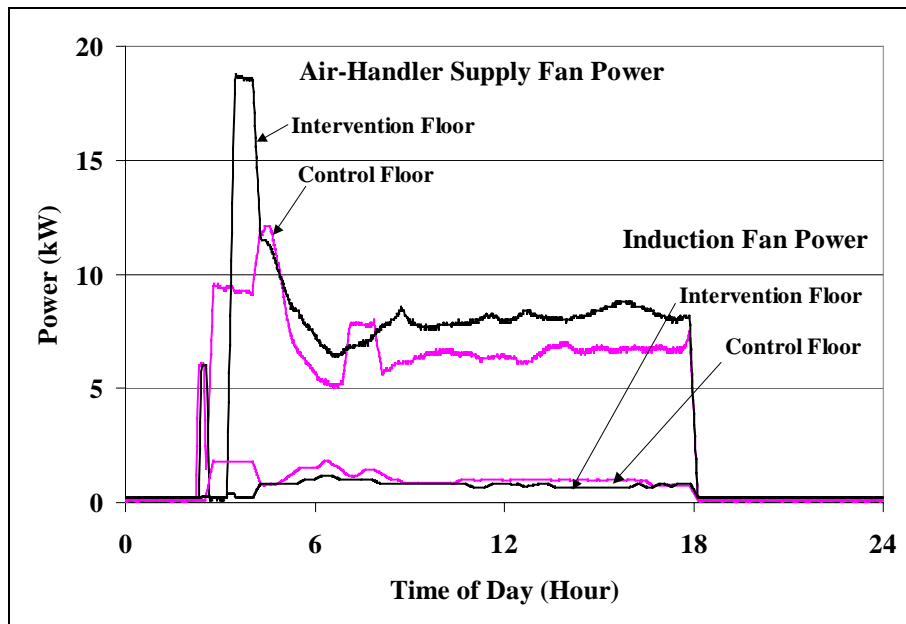


Figure II-14. Air-handler supply fan and induction fan power for a sample “Up & Down” day.

References

Franconi, E., W. Delp, and M. Modera. 1998. "Impact of Duct Air Leakage on VAV System Energy Use". Draft Report, Lawrence Berkeley National Laboratory, Berkeley, CA. LBNL 42417.

SMACNA. 1985. "HVAC Air Duct Leakage Test Manual". Chantilly, VA: Sheet Metal and Air Conditioning Contractors National Association, Inc.

Walker, I.S., C.P. Wray, D.J. Dickerhoff, and M.H. Sherman. 2001. "Evaluation of Flow Hood Measurements for Residential Register Flows". Lawrence Berkeley National Laboratory. Berkeley, CA. LBNL-47382.

Wray, C.P., I.S. Walker, and M.H. Sherman. 2002. "Accuracy of Flow Hoods in Residential Applications". Proc. ACEEE Summer Study 2002. Vol. 1, pp. 339-350. American Council for an Energy Efficient Economy, Washington, DC. LBNL-49697.

Xu, T., M. Modera, R. Carrie, D. Wang, D. Dickerhoff, and J. McWilliams. 2002. "Commercial Thermal Distribution Systems: Performance Characterization and Aerosol-Sealing Technology Development". Draft Final Report for the U.S. Department of Energy, Lawrence Berkeley National Laboratory, Berkeley, CA. LBNL-46283.